CHEMICAL ENGINEERING TRANSACTIONS
VOL. 43, 2015
A publication of AIDIC
The Italian Association of Chemical Engineering
Online at www.aidic.it/cet
Chief Editors: Sauro Pierucci, Jiří J. Klemeš

ISBN 978-88-95608-34-1; **ISSN** 2283-9216
DOI: 10.3303/CET1543194

Sensibility Study of the Reynolds Stress Model Parameters for Swirling Flows in Cyclones

Evandro Balestrin*, Rafaello D. Luciano, Dirceu Noriler, Rodrigo K. Decker, Henry F. Meier

University of Blumenau, São Paulo St., 3250, Room I-204, 89030-000, Blumenau-SC, Brazil
evandrobalestrin@hotmail.com

Several studies found in the literature apply Computational Fluid Dynamics (CFD) for the swirling flow in cyclones, such as Costa et al. (2013) who studied solid-solid interactions, and Sgrott Jr. et al. (2013) that investigated a technique for cyclones' project optimization. The main characteristic of this flow is the anisotropic behavior of the turbulence due to the highly swirling gas flow. In this sense, a turbulence model with capability to predict the swirling flow, such as the Reynolds Stress Model (RSM), must be applied. This model has been used in numerous studies of cyclones and the results showed that the model is well suited to predict the pressure drop and the axial velocity component of the flow. However, for the tangential velocity component the results were not satisfactory for quantitative validation. Based on a comparison of numerical and experimental results, and knowing the importance of the axial and the tangential velocities for the efficiency of collection in cyclones and for the pressure drop, the latter which is related to energy costs; the main objective of this study is to present a sensibility study of the Reynolds Stress Model parameters for swirling flow in cyclones. To perform this study, a CFD commercial code was used to simulate cases based on a 2^{n-3} factorial design. In this design, seven parameters of the RSM-SSG model (C1, C1*, C2, C3, C3*, C4 and C5) were varied 5% above and below their standard values in order to analyze the effect of each parameter in the pressure drop and in the axial and tangential velocity profiles in cyclones for the gas phase flow. The results showed that the parameters C1 and C1* have more influence in the pressure drop and the parameters C3 and C3* have more influence in the axial and tangential velocity peaks.

1. Introduction

Cyclones are simple devices with no moving parts. They basically consist of a cylindrical and conical body, a cover plate with an immersion tube and a tangential inlet. The principle of cyclone work is based on the centrifugal force that redirects the solid particles towards the wall, and on the high turbulent intensity that produces reversed gas flow. Cyclones are applied in several separation processes such as gas-solid; they are widely used in cement, chemicals and petro-chemicals industries due to low maintenance cost and high efficiency of separation in normal and elevated temperatures and pressures.
In general, the fluid dynamics problems can be approached in two ways, experimental methods or numerical methods. In this work, fluid dynamics phenomena in cyclones were approached with numerical methods.
To study the fluid dynamics phenomena with numerical methods it is necessary to solve the equations that govern it, using CFD. However, most practical applications of computational fluid dynamics require the use of a turbulence closure model. In this sense, a turbulence closure model with capability to predict the swirling flow was applied, the Reynolds Stress Model (RSM). This model has been validated and used in numerous studies of cyclones and the results showed that the model is well suited to predict some parameters connected to cyclone's performances, such as pressure drop, axial velocity and tangential velocity by the qualitative point of view.
Many CFD studies have confirmed the application of the RSM to predict the swirling gas flow in cyclones, such as Noriler et al. (2004) who studied a device for pressure drop reduction, Ropelato et al. (2010) that investigated

Please cite this article as: Balestrin E., Luciano R., Noriler D., Decker R.K., Meier H., 2015, Sensibility study of the reynolds stress model parameters for swirling flows in cyclones, Chemical Engineering Transactions, 43, 1159-1164 DOI: 10.3303/CET1543194

CFD practices on cyclones, El-Batsh (2012) that studied cyclones' exit pipe and Balestrin et al. (2014) who validated this model through physical experimentation. In some cases the authors needed to change the standard RSM parameters to better adjust to the experimental results; Buss et al. (2012) made a parametrical sensibility analysis of the Reynolds Stress Model in a coaxial and confined jet flow. Therefore, this work aims to present a sensibility study of seven of the Reynolds Stress Model parameters over the pressure drop, axial velocity and tangential velocity in cyclones.

2. Materials and Methods

To perform this parametrical sensibility study, a 2^{n-3} factorial design was made and a CFD commercial code was used to simulate all cases.

2.1 Factorial Design

The factorial design and the analyses of the results were performed in STATISTICA 7.0 software. To produce the factorial design, seven parameters of the RSM-SSG model (C1 = 3.4, C1* = 1.8, C2 = 4.2, C3 = 0.8, C3* = 1.3, C4 = 1.25 and C5 = 0.4) were varied 5% above and below of their standard values. This design was made to analyze the effect/significance of each parameter in the pressure drop, and in the axial and tangential velocity profiles in the inner sections of the cyclones for the flow of the gas phase. The 2^{7-3} factorial design generated seventeen different cases that were used to perform the numerical experiments.

2.2 Numerical Simulation

Numerical simulations were performed in a CFD commercial code, FLUENT 14.0 from ANSYS. This code uses the finite volumes method to discretize the set of partial differential equations of the mathematical model. The geometry used in the numerical simulations consists of a cyclone with 294 mm diameter and 520 mm height, linked with a collector box and a set of inlet and outlet pipes, such as shown in Figure 1. In this study, the simulations were performed in a hexahedral mesh with about 1 millions points (1,147,218 points).
The main settings used in the commercial code to simulate the swirling gas flow were: RSM-SSG as turbulence closure model, SIMPLEC as the method for pressure-velocity coupling, PRESTO for the pressure`s spatial discretization and Second Order Upwind for the momentum`s spatial discretization. The gas velocity in the inlet pipe was 10.5 m/s and in the inlet of the cyclone, it was about 12 m/s.

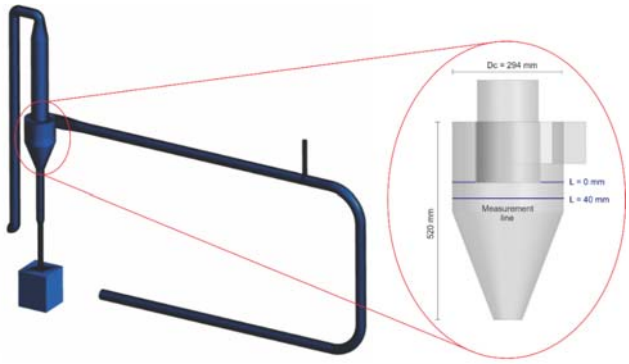

Figure 1: geometry used in the simulations and illustration of the measurement line of the axial and tangential velocity profiles (L = 40 mm) in the inner of cyclone.

3. Mathematical Modelling

The mathematical model applied in this study is based on the Reynolds-Averaged-Navier Stokes equations with an Eulerian-Eulerian approach, as follows:

Mass conservation equation,

$$\frac{\partial}{\partial t}(\rho_g) + \boldsymbol{\nabla} \cdot (\rho_g \boldsymbol{v_g}) = 0\,. \tag{1}$$

Momentum equations,

$$\frac{\partial}{\partial t}(\rho_g \boldsymbol{v}_g) + \boldsymbol{\nabla} \cdot (\rho_g \boldsymbol{v}_g \boldsymbol{v}_g) = -\boldsymbol{\nabla} \cdot (\boldsymbol{T}_g^{eff}) + \rho_g \boldsymbol{g} - \boldsymbol{\nabla} p\,. \tag{2}$$

Where the subscript “g” represents the gas phase and the effective tensor can be defined as the sum between the Reynolds turbulent tensor ($\mathbf{T}_g^t$) and the molecular tensor($\mathbf{T}_\mathrm{g}$):

$$\boldsymbol{T}_g^{eff} = \boldsymbol{T}_g^t + \boldsymbol{T}_g \,. \tag{3}$$

For the turbulence closure equations, the Reynolds Stress Model (RSM) was applied:

$$\frac{\partial}{\partial \mathrm{t}}\left(\rho_\mathrm{g}\boldsymbol{T}_g^t\right) + \boldsymbol{\nabla}\cdot\mathbf{v}_\mathrm{g}\left(\rho_\mathrm{g}\boldsymbol{T}_g^t\right) = \mathbf{D}_\mathbf{T} + \mathbf{D}_\mathbf{M} + \boldsymbol{\Upsilon} + \boldsymbol{\Pi} - \frac{2}{3}\boldsymbol{\delta}\rho_\mathrm{g}\varepsilon_\mathrm{g}\,. \tag{4}$$

The turbulent diffusion ($\mathbf{D}_\mathbf{T}$) must be modeled as:

$$\mathbf{D}_\mathbf{T} = \boldsymbol{\nabla}\cdot\left(\frac{\mu_g^t}{\sigma_k}\boldsymbol{\nabla}\mathbf{T}_g^t\right). \tag{5}$$

The molecular diffusion ($\mathbf{D}_\mathbf{M}$) and the production rate ($\boldsymbol{\Upsilon}$) are expressed as:

$$\mathbf{D}_\mathbf{M} = \boldsymbol{\nabla}\cdot\left(\mu\boldsymbol{\nabla}\mathbf{T}_g^t\right); \tag{6}$$

$$\boldsymbol{\Upsilon} = -\rho_\mathrm{g}\left[\mathbf{T}_g^t\cdot\left(\boldsymbol{\nabla}\mathbf{v}_\mathrm{g}\right)^\mathrm{T} + \mathbf{T}_g^t\cdot\left(\boldsymbol{\nabla}\mathbf{v}_\mathrm{g}\right)\right]. \tag{7}$$

The deformation rate due to pressure ($\boldsymbol{\Pi}$) was divided in three parts for better visualization of each term and it can be defined in different ways. In this study, the quadratic modeling proposed by Speziale, et al.(1991) was applied. This model is represented as RSM-SSG and can be expressed as:

$$\boldsymbol{\Pi} = \boldsymbol{\Pi}_\mathbf{1} + \boldsymbol{\Pi}_\mathbf{2} + \boldsymbol{\Pi}_\mathbf{3}\,. \tag{8}$$

Where:

$$\boldsymbol{\Pi}_\mathbf{1} = -\rho_\mathrm{g}\varepsilon_\mathrm{g}\left[\mathrm{C}_1\boldsymbol{b} + \mathrm{C}_2\left(\mathbf{b}\cdot\mathbf{b} - \frac{1}{3}\mathbf{b}:\mathbf{b}\boldsymbol{\delta}\right)\right]; \tag{9}$$

$$\boldsymbol{\Pi}_\mathbf{2} = -C_1^*\Upsilon^*\boldsymbol{b} + \rho_\mathrm{g}k_g\boldsymbol{S}\left(\mathrm{C}_3 - C_3^*\sqrt{\mathbf{b}:\mathbf{b}}\right); \tag{10}$$

$$\boldsymbol{\Pi}_\mathbf{3} = +\mathrm{C}_4\rho_\mathrm{g}k_\mathrm{g}\left(\boldsymbol{b}\cdot\boldsymbol{S}^\mathrm{T} + \boldsymbol{S}\cdot\boldsymbol{b}^\mathrm{T} - \frac{2}{3}\boldsymbol{b}:\boldsymbol{S}\boldsymbol{\delta}\right) + \mathrm{C}_5\rho_\mathrm{g}k_\mathrm{g}\left(\boldsymbol{b}\cdot\boldsymbol{\Omega}^\mathrm{T} + \boldsymbol{\Omega}\cdot\boldsymbol{b}^\mathrm{T}\right). \tag{11}$$

For the solution of the deformation rate due to pressure it is necessary to define three other equations for: the Reynolds anisotropic tensor (***b***), the deformation rate (**S**) and the vorticity (**Ω**), as follows:

$$\boldsymbol{b} = \frac{\mathbf{T}_g^t}{\mathrm{k}_\mathrm{g}} - \frac{2}{3}\boldsymbol{\delta}\,; \qquad \mathbf{S} = \frac{1}{2}\left[\boldsymbol{\nabla}\mathbf{v}_\mathrm{g} + \left(\boldsymbol{\nabla}\mathbf{v}_\mathrm{g}\right)^\mathrm{T}\right]; \qquad \boldsymbol{\Omega} = \frac{1}{2}\left[\boldsymbol{\nabla}\mathbf{v}_\mathrm{g} - \left(\boldsymbol{\nabla}\mathbf{v}_\mathrm{g}\right)^\mathrm{T}\right]. \tag{12}$$

The turbulent kinetic energy (k) is represented by the trace of the Reynolds tensor, although a transport equation can be attributed to it. The dissipation rate (ε) requires a conservation expression as:

$$\frac{\partial}{\partial t}\left(\mathrm{f}_\mathrm{g}\rho_g\varepsilon_g\right) + \boldsymbol{\nabla}\cdot\left(\mathrm{f}_g\rho_g\mathbf{v}_\mathrm{g}\varepsilon_\mathrm{g}\right) = \boldsymbol{\nabla}\cdot\left[\left(\mu - \frac{\mu_g^t}{\sigma_\varepsilon}\right)\boldsymbol{\nabla}\varepsilon_g\right] + \frac{1}{2}\frac{\varepsilon_g}{\mathrm{k}_g}\mathrm{f}_g\mathrm{C}_{\varepsilon1}\Upsilon^* - \frac{{\varepsilon_g}^2}{\mathrm{k}_g}\mathrm{f}_g\rho_g\mathrm{C}_{\varepsilon2}\,. \tag{13}$$

The turbulent viscosity (μ_g^t) is represented by:

$$\mu_g^t = \rho_\mathrm{g}\mathrm{C}_\mu\frac{{\varepsilon_\mathrm{g}}^2}{\mathrm{k}_\mathrm{g}}. \tag{14}$$

The commonly constant values applied in this model are: σ_k= 0.82, C_1= 3.4, C_1^*= 1.8, C_2= 4.2, C_3= 0.8, C_3^*= 1.3 C_4= 1.25, C_5= 0.4, σ_ε= 1.0, $\mathrm{C}_{\varepsilon1}$= 1.44, $\mathrm{C}_{\varepsilon2}$= 1.88.

4. Results and Discussion

The main tools used when analyzing the variation that the parameters impose on the velocity profiles and on the pressure drop were the fitted response surface plots and the Pareto chart analyses. It was decided to analyze the axial and tangential velocity results in some points that were located in order to evaluate critical areas in the velocity profiles. These critical points were chosen based on a comparison of numerical results and experimental data obtained with PIV techniques. The effects of the seven RSM-SSG parameters in the axial velocity and tangential velocity were analyzed in the points shown in Figure 2 (a) and Figure 2 (b). The figure also shows the variation observed in the velocity profiles for all cases specified in the factorial design and the experimental results.

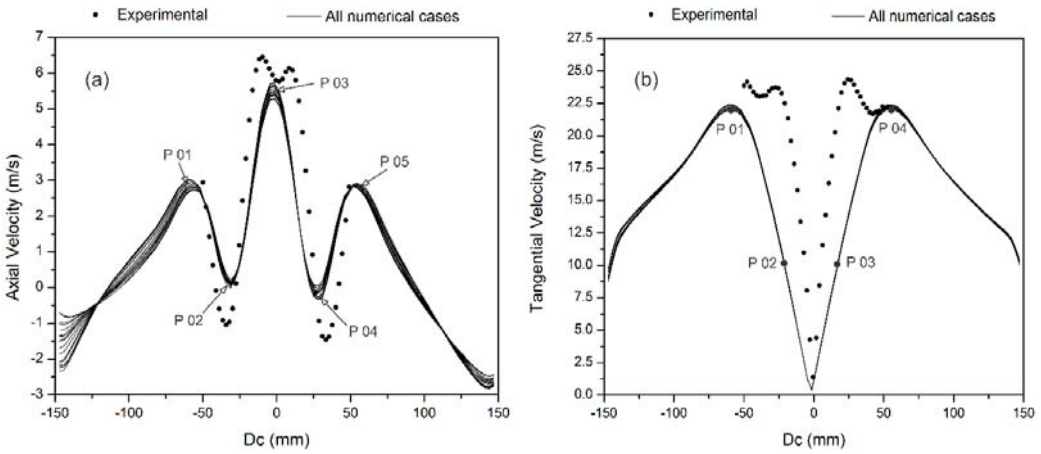

Figure 2: comparison between numerical and experimental data, and position of the points analyzed in the velocity profiles: (a) axial velocity; (b) tangential velocity.

Analyzing all numerical cases, a significant variation was observed in the axial velocity profile at the critical points (Figure 2 (a)), but a bigger deviation of the parameters is suggested in order to better study a numerical representation of the experimental data. On the other hand, points 02 and 03 in Figure 2 (b) did not show as much movement towards the experimental data. This difficulty of the RSM-SSG model to predict the tangential velocity peaks, and the displacing of the peaks to closer to the walls, as seen on Figure 2 (b), was also observed by other authors, such as Peres et al. (2001).

4.1 Axial Velocity

In Figure 3 (a) it is possible to be observed that parameters C3, C3* and C4 directly affect the velocity value in point 03, with 95% confidence. These parameters are located in the second and in the third term of the deformation rate due to pressure (Eq(10) and Eq(11)). Analyzing the signals we can notice that increasing C3 or C4 tends to increase the velocity value in that position, while increasing C3* decreases it. The chart in Figure 3 (b) confirms those notions, in this fitted response surface it is possible to be noticed that increasing either C3 or C4, the axial velocity value also increases in the evaluated position.

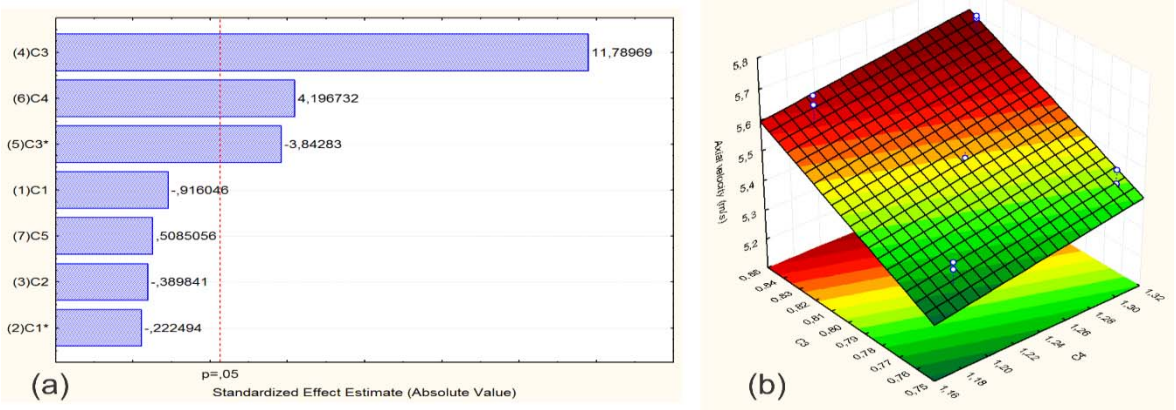

Figure 3: axial velocity results in point 03: (a) Pareto chat; (b) fitted response surface.

For points 01 and 04, the relevant parameters were mainly C3, C3* and C4, as shown in Figure 4. Observing Figure 4 (a), when the value of C3 and C4 are increased, the axial velocity tends to decrease in these positions, while increasing C3* tends to decrease them. Analyzing Figure 4 (b), it is possible to be noticed that by increasing the value of C3 or C4 the axial velocity decreases, while increasing C3* the axial velocity also tends to increase. The behavior of the points 02 and 05 are the same as points 01 and 04, respectively.

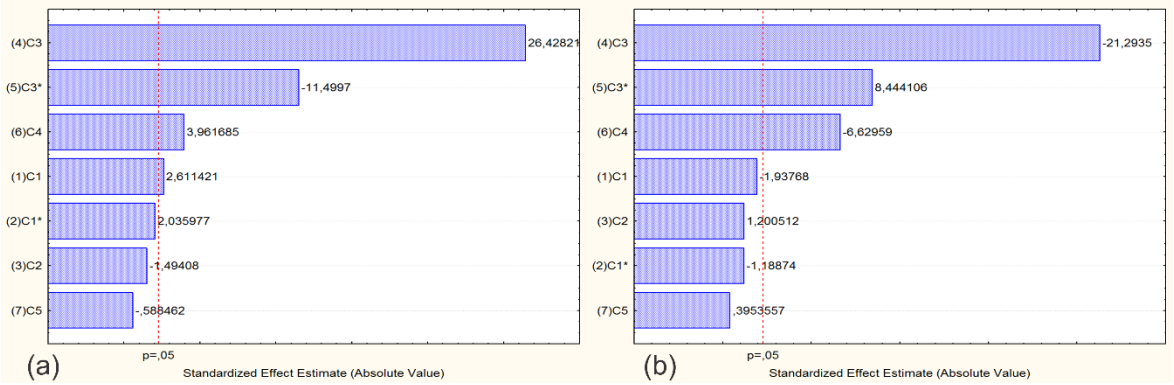

Figure 4: pareto chart for axial velocity results: (a) point 01; (b) point 04.

4.2 Tangential Velocity

Analyzing the Figure 5 (a) , it is possible to be concluded that the parameters C3 and C3* are the ones that affected the tangential velocity the most in point 01, and with 95% of confidence it is correct to be inferred that this position's velocity value is directly affected by parameters C1, C1*, C4, C3* and C3. It can also be stated, by analyzing the signals of the values, that by increasing C3 the velocity peak in which point 01 is located increases; whereas by increasing C3* the velocity peak decreases. Figure 5 (b) confirms this observation.

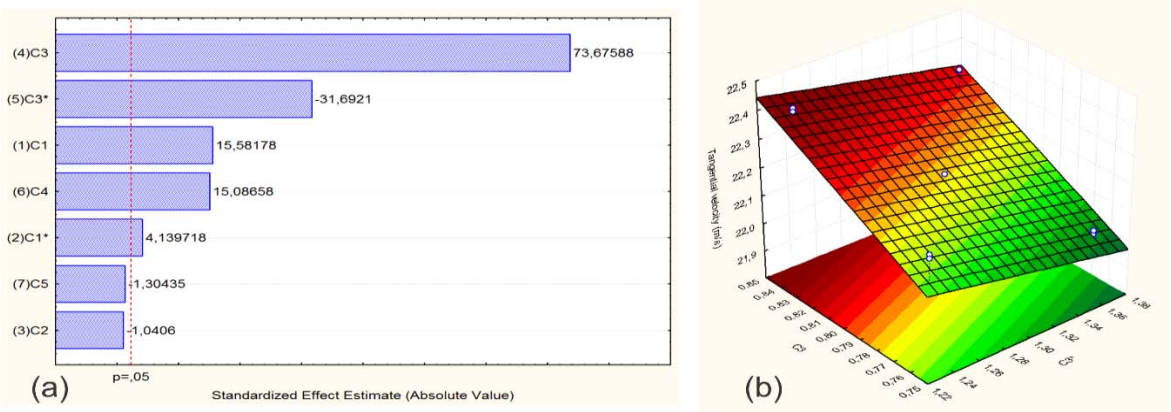

Figure 5: tangential velocity results in point 01: (a) Pareto chat; (b) fitted response surface.

In Figure 5 (b), the left vertical axis represents the predicted tangential velocity in meters per second for the point being analyzed, while the horizontal axes represent the parameters. The left horizontal axis is C3 while the right one is C3*. When increasing parameter C3, the velocity increases, while increasing C3*, it decreases. This exact same behavior is noticed for point 04.

For points 02 and 03, making the same analysis, C3 and C3* were the significant parameters with 95% of confidence, but their effects were less noticeable.

4.3 Pressure Drop

Figure 6 (b) presents the parameters that have significance for the pressure drop results in the cyclone. As seen, the relevant parameters were C1 and C1*, with both promoting positive variation on it, or in other words, increasing either one tends to increase the pressure drop of the simulated cyclone. This observation is better visualized in Figure 6 (b). Parameters C1 and C1* are located in the first and in the second term of the deformation rate due to pressure (Eq(9) and Eq(10)).

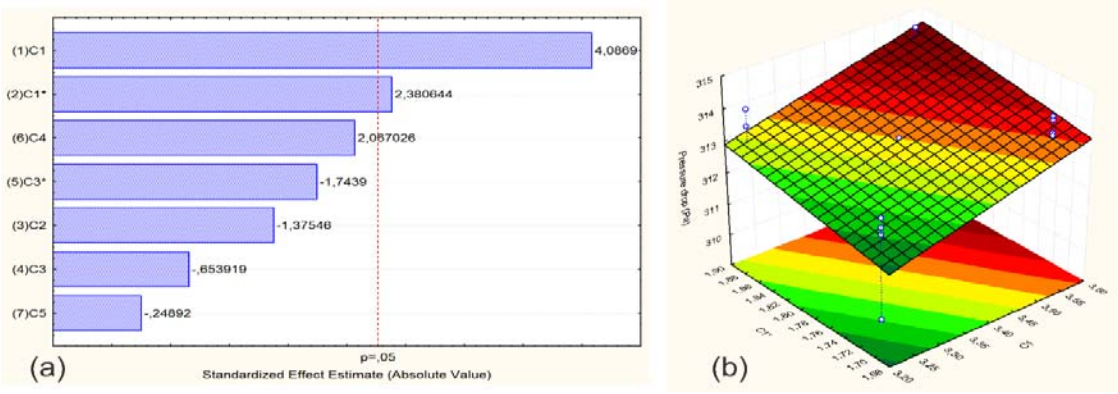

Figure 6: pressure drop results: (a) Pareto chat; (b) fitted response surface.

5. Conclusions

Trends were noticed when analyzing the sensibility of RSM-SSG parameters. The main one is that C3 generally affects all the peaks of both tangential and axial velocity profiles, increasing their amplitudes or to put it in another way further increasing high peaks and at the same time decreasing low or negative peaks. Also, C3* seems to affect all the peaks as well, with its effect being the opposite of C3. The parameters that significantly affected the pressure drop in cyclone flow were C1 and C1*, with both having a positive effect on it. Therefore, to better represent the experimental data with the numerical results it is suggested to adjust parameters C3 and C3* for the velocity profiles, and C1 and C1* for the pressure drop. Also, as a suggestion for future work, a bigger deviation of the most important parameters is advised in order to better observe their effects.

Acknowledgements

The authors are grateful to PETROBRAS and CNPQ for the financial support that made this work possible.

References

Balestrin E., Sgrott Jr. O. L., Decker R. K., Wiggers V. R., Meier H. F., 2014, Application of Numerical and Experimental Techniques for Verification and Validation in Cyclones, 2014 AIChE Annual Meeting, 594b, Atlanta, GA, USA.

Buss L., Decker R. K., Meier H. F., 2012, Parametrical Sensibility Analysis of Reynolds Stress Model in a Coaxial and Confined Jet Flow, 2012 AIChE Annual Meeting, 320g, Pittsburgh, PA, USA.

Costa K. K., Sgrott Jr. O. L., Decker R.K., Reinehr E. L., Martignoni W. P., Meier H. F, 2013, Effects of Phases' Numbers and Solid-Solid Interactions on the Numerical Simulations of Cyclones, Chemical Engineering Transactions, 32, 1567-1572, DOI:10.3303/CET1332262

El-Batsh H. M., 2012, Improving Cyclone Performance by Proper Selection of the Exit Pipe, Applied Mathematical Modelling, 37, 5286-5303.

Noriler D., Vegini, A. A., Soares C., Barros A. A. C., Meier H. F., Mori M. A., 2004, A New Role for Reduction in Pressure Drop in Cyclones Using Computational Fluid Dynamics Techniques, Brazilian Journal of Chemical Engineering, Brazil, 21, 93-101.

Peres A. P., Meier H. F., Kasper F. R. S., Huziwara W. K., Mori M., 2001, Analysis of Turbulence Models and Importance of Grid Refinement in 3-D Simulation of Gas Flow in a Cyclone, 16th Brazilian Congress of Mechanical Engineering, 8, 79-87.

Ropelato K., Fontes C. E., Fusco J. M., 2010, On CFD practices for cyclone simulation, 7th International Conference on Multiphase Flow, Tampa, FL, USA.

Sgrott Jr. O. L., Costa K. K., Noriler D., Wiggers V. R., Martignoni W. P., Meier H. F., 2013, Cyclones' Project Optimization by Combination of an Inequality Constrained Problem and Computational Fluid Dynamics Techniques (CFD), Chemical Engineering Transactions, 32, 2011-2016, DOI:10.3303/CET1332336

Speziale C. G., Sarkar S., Gatski T. B., 1991, Modelling the Pressure-Strain Correlation of Turbulence: An Invariant Dynamical Systems Approach, Journal Fluid Mechanics, 227, 245–272.